A PRECISE FORCE MEASUREMENT IN MAGNETIC BEARINGS FOR DIAGNOSIS PURPOSES

M. Aenis, R. Nordmann
Darmstadt, University of Technology
Department of Mechatronics
aenis@mesym.tu-darmstadt.de
nordmann@mesym.tu-darmstadt.de

ABSTRACT

The aim of the presented project sponsored by the DFG (German Research Council) is to use active magnetic bearings for the diagnosis of centrifugal pumps. Therefore, active magnetic bearings are integrated in a single-stage respectively four-stage pump substituting the conventional ball bearings. The diagnosis procedures are based on evaluating frequency response functions where the active magnetic bearings operate as actuators and as sensors to measure the displacements and the forces induced in the rotating structure. Simulation results of an exemplarily fault applied to the pump system are presented.

For this type of diagnosis using transfer functions, an accurate force measurement is crucial. The paper compares force measurement results and achievable accuracies of a radial magnetic bearing using different measurement techniques over a large operating range. Furthermore, a finite-element model is used to investigate fringing and leakage effects to improve the different measurement techniques. The finite element model allows eccentric rotor positions and non-symmetrical coil current distributions with nonlinear material properties of the stator and rotor part of the magnetic bearing.

INTRODUCTION

Nowadays, the industrial applications of turbomachines demand higher reliability and availability. Therefore, an integrated failure detection becomes increasingly more important in the case of these machines.

Up to now, the monitoring systems are normally not an integral component of turbomachines. They must be additionally acquired by the operators of such machines. In the case of these failure detection systems, the relative and/or absolute motions of the rotor are measured as output signals. After signal processing, certain features (threshold values, orbits, frequency spectra and so forth) are created from the measured data. With the deviations of these features from a faultless initial state, the diagnosis attempts to recognize possible faults. The problem with these procedures is that the causes of the modifications of the

output signal can not be detected clearly. They can either lie in a change of the process or in a modification of the system itself.

An improvement of the existing diagnostic techniques is possible through the use of active magnetic bearings (AMB) in turbomachines (fig. 1). The active magnetic bearings are able to excite rotating shafts without contact and to measure simultaneously the required forces and displacements very precisely. Consequently, frequency response functions (stiffness or compliance frequency responses) can be determined from the measured input and output signals, of which the physical parameters (mass, damping, stiffness) or modal parameters (natural frequencies, eigenmodes, modal damping) of the system are identified.

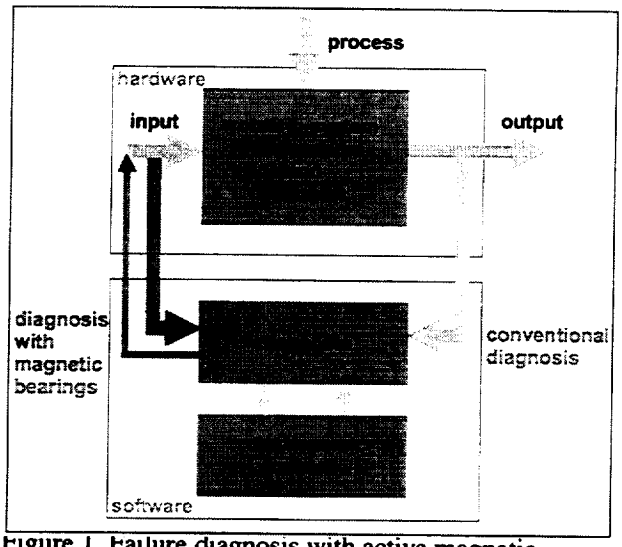

Figure 1. Failure diagnosis with active magnetic bearings.

In the presented project of the Special Research Program (SFB 241) supported by the German Research Council (DFG), it is examined how faults in turbomachines can be diagnosed experimentally with active magnetic bearings. An important role of the development of the fault diagnosis is the precise measurement of the input/output values (motions and forces). The measurement of the displacements by means of the utilised Eddy current probes have reached a sufficient precision. That is not the case for the measurement of the forces applied to rotating structures. In the following, results of different force measurements using magnetic bearings (i-s-method, reluctance network method, Hall sensor method) are compared.

Afterwards, the method of the model based diagnosis is then presented briefly by means of simulation of a selected fault applied to the single-stage pump representing the turbomachine system. Parallel to the numeric computations, a test rig of the single-stage pump (fig. 2) is under construction. This test rig is used to verify and to demonstrate the performance of the developed diagnosis methods. The pump is located between two active magnetic bearings levitating

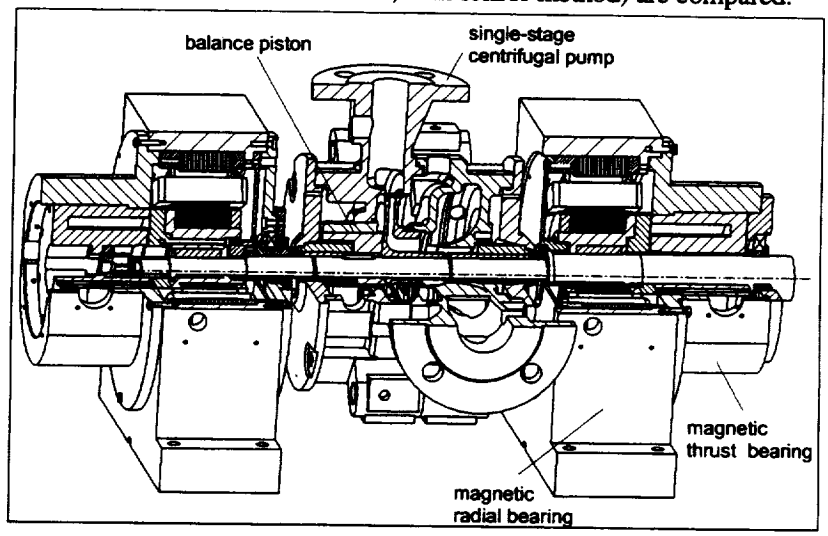

Figure 2. Scheme of the test rig of the single-stage centrifugal pump in active magnetic bearings.

the rotor in five degrees of freedom. Besides the replacement of the conventional roller bearings with the active magnetic bearings, the original pump system remains unchanged. In addition to the two mechanical seals sealing up the hydraulic part, the pump contains two contactless annular seals. One is placed at the suction side and one at the pressure side of the impeller, which is the balance piston. The modular design of the test rig enables an easy extension of the single-stage to a four-stage pump system for future investigations.

FORCE MEASUREMENT WITH MAGNETIC BEARINGS

Description of the Active Magnetic Bearings

Unlike conventional bearing systems, the rotor is carried by a magnetic field. In this case, sensors and controllers are necessary to stabilize the unstable open loop state of the rotor. Therefore, essential dynamic characteristics like stiffness and damping properties are influenced by the controller. The rotor can be moved on almost arbitrarily chosen trajectories independently of the rotation. These can either be harmonic motions in one plane, forward or backward whirls. Additionally, an imbalance compensation can be performed.

A magnetic bearing system consists of four basic components: magnetic actuator, controller, power amplifier, and shaft position sensor. To keep the rotor in the bearing center, the position sensor signal is used as input for an electronic control circuit to adequately adjust the coil currents. As shown in fig. 3, the stator component is normally composed of horseshoe-shaped magnets and the rotor component is a ring

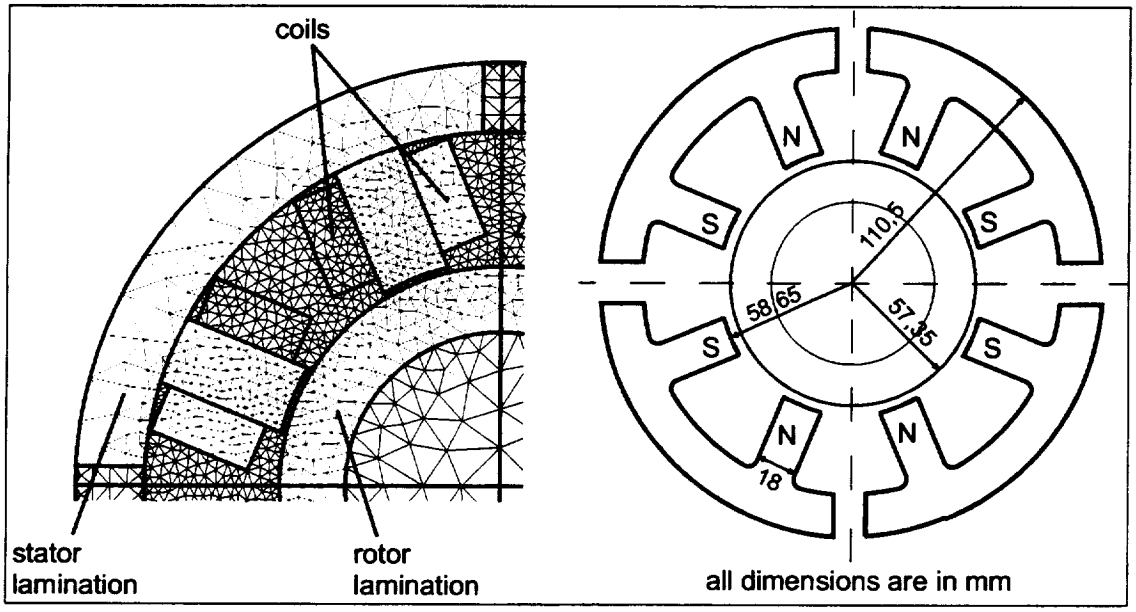

Figure 3. FE-Model and the main dimensions of the stator and rotor laminations of the magnetic bearing.

of magnetic material to complete the magnetic path. The bearing configuration is operated in the so-called differential driving mode [10], where one magnet is driven with the sum of bias current i_0 and control current i_x, and the other one with the difference. Consequently, if the magnetization of the iron is neglected, a linear force-current-displacement relation is obtained. The operation point of the magnetic bearing is determined by the bias current (here $i_0 = 4A$), which is half of the maximum coil current. Figure 3 shows the main geometric data of the bearings used. The material carrying the magnetic flux consists of SiFe-laminations with typically nonlinear soft magnetic material behavior.

Force-Current-Displacement Characteristic of the Magnetic Bearings

The setup for the measurements to compare the different measurement techniques is shown in figure 4 and is explained in detail in the work done by Knopf et al. [6]. An external load cell is used to obtain a reference force F_{ref}. While the rotor is floating in the active magnetic bearings, different external static forces F_{ref} are applied (starting with positive maximum force until negative and back). This procedure is performed for different rotor positions. The data of the external forces, coil currents, and rotor positions are recorded simultaneously. Figure 5 shows the resulting measured static force-current-displacement characteristic for one axis of the radial magnetic bearing. Dynamic effects like eddy currents are neglected in this paper and will not be considered in the following.

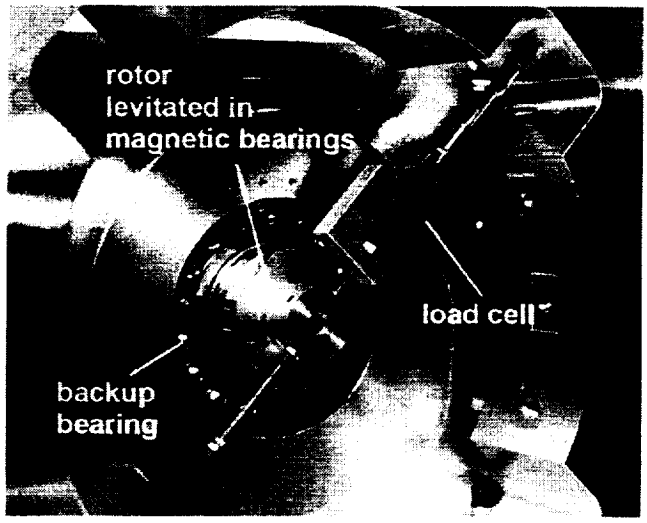

Figure 4. Setup for the force measurement of the external loads applied to the levitated rotor.

The necessary magnetic bearing forces F_{AMB} to compensate the externally applied forces F_{ref} are determined in different ways. In general, the magnetic force F_{AMB} can be computed from

$$F_{AMB} = \frac{A_{pole}}{2\mu_0} \sum_k B^2_{pole_k}, \tag{1}$$

assuming a uniform flux density in every flux-carrying cross-section and no flux fringing at the tip of the poles. In equation (1), A_{pole} stands for the cross-section of the poles carrying the flux densities B_{pole_k}. Where B_{pole_k} are the fluxes at the different magnetic poles. μ_0 means the magnetic permeability of vacuum. Hence, the entire force of the radial bearing results from the sum of the individual forces of each pole.

i-s-Method

Using magnetic bearings in differential driving mode [10], equation (1) can be linearized leading to the well-known equation

$$F_x = k_i i_x + k_s s_x \tag{2}$$

where i_x is the control current in the x-direction, s_x is the rotor displacement in the x-direction, and N represents the number of coil turns. The linearization constants k_i, k_s depend on the chosen design point of the magnetic bearings (i_0, s_0) and are computed using the following equations

$$k_i = \frac{\mu_0 N^2 A_{Pole} \cos(\pi/8) i_0}{s_0^2} \tag{3}$$

$$k_s = \frac{\mu_0 N^2 A_{Pole} (\cos(\pi/8))^2 i_0^2}{s_0^3}. \tag{4}$$

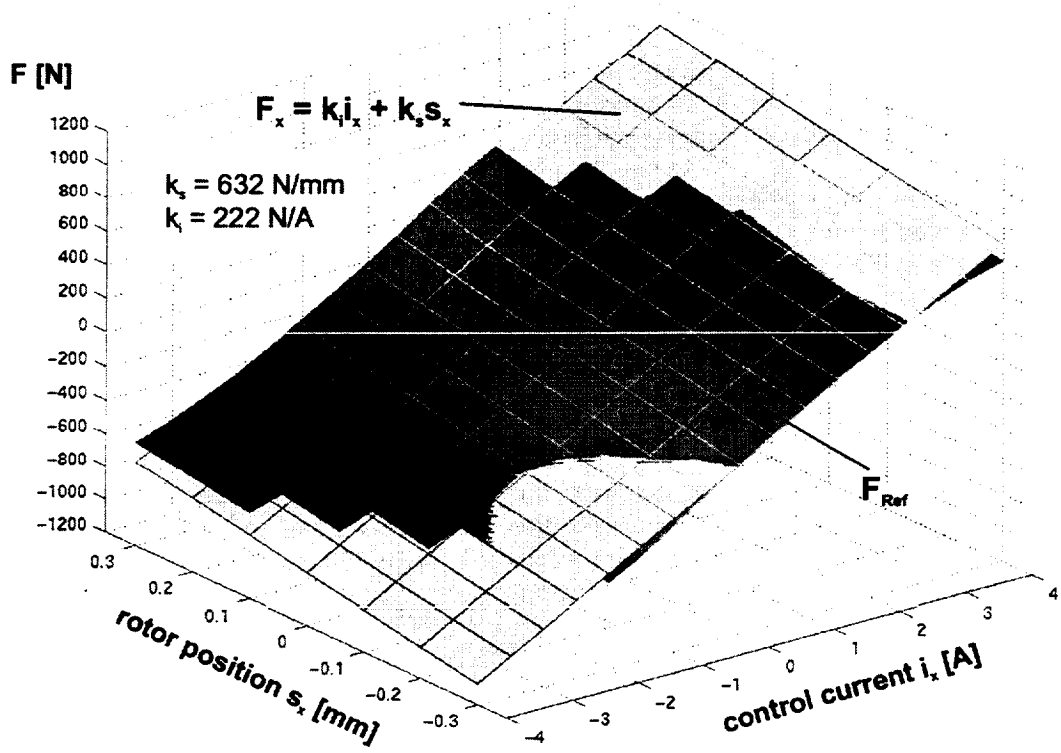

Figure 5. Measured and linearized force-current-displacement characteristic for one magnetic bearing axis.

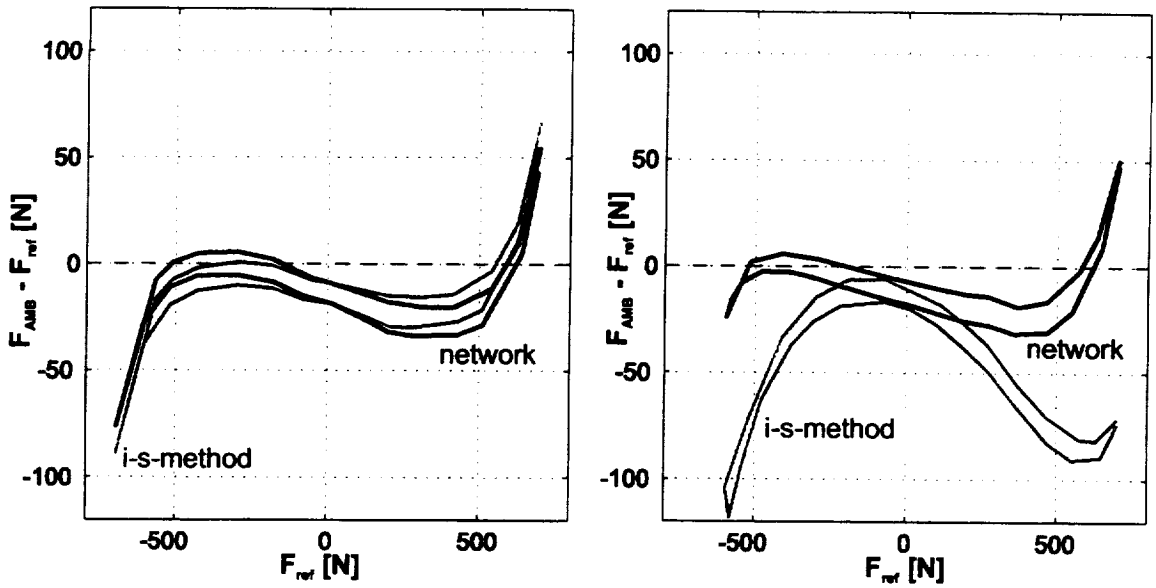

Figure 6. Force error of the i-s-method and network method without calibration for a centric (=0mm, s_y=0mm) and an eccentric (s_x=0.3mm, s_y=0mm) rotor position.

Figure 5 shows the linearized force-current-displacement characteristic using equation (2) with the analytically computed k_i-k_s-values. This method assumes a uniform flux density in the air gap and neglects flux paths in the iron part, fringing and leakage effects.

The resulting force error of the i-s-method is demonstrated in figure 6 for a centric rotor position (s_x=0mm, s_y=0mm) and for an eccentric rotor position (s_x=0.3mm, s_y=0mm). In case of a centric rotor position, the error significantly increases with high external loads due to the nonlinear material properties (BH-curve) which are neglected with this method. Furthermore, the influence of the hysteresis of the soft magnetic material behavior can be seen, which results in a splitting up of 10N. The right side of figure 6 shows the significant dependence of the force error on the rotor position due to the neglected nonlinear material behavior and additional fringing effects.

Summarizing, in an operating range of ±0.3mm (that is 23% of the nominal air gap) and ±700 N (that is 100% of the maximum bearing force) the force error calculated with the i-s-method is about 17%. An increase in the accuracy can be reached with calibration, which is performed with a least-square fit of the k_i-k_s-plane to the measured data. The resulting value for k_i is 217 N/A and for k_s is 759 N/mm. Then, the force error of the chosen operating range is less than 9%. Figure 7 shows the corresponding force errors after calibration for the same two rotor positions. It should be mentioned that the calibration of k_i, k_s is strongly dependent on the chosen operating range. By limiting the working range of the bearings, the accuracy of the measurement method could be increased.

The i-s-method is simple and often used for on-line computation of the magnetic bearing forces because information about the coil currents and rotor positions is available during digital control and no additional sensors are needed. The disadvantage of the i-s-method is the neglect of the material properties of iron, leakage and fringing effects.

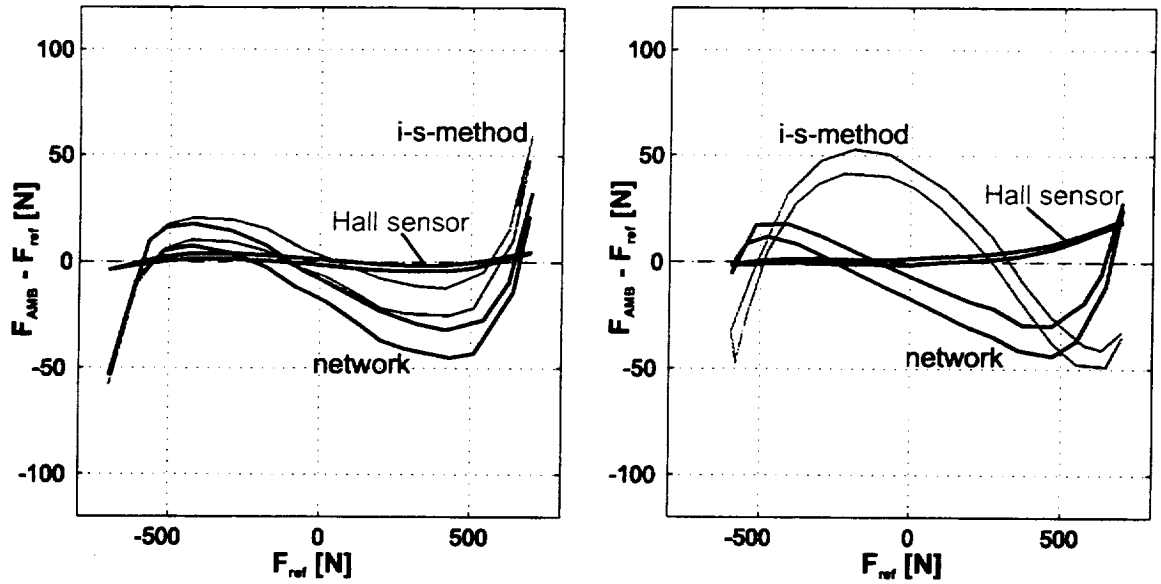

Figure 7. Force error of the different force measurement methods with calibration for a centric (s_x=0mm, s_y=0mm) and an eccentric (s_x=0.3mm, s_y=0mm) rotor position.

Reluctance Network Model

The second force measurement method is based on a reluctance network. The entire bearing is modelled as a multi-node network of variable reluctances (air gaps, pole legs, and back-iron paths of the stator) located between the model node points as it is described in Gähler [3]. Magnetic networks can be computed in a similar way to electric networks. The magnetic flux Φ corresponds to the electric current i and the magnetic potential ($\Delta V = Ni$) to the electric voltage U. The reluctance is then similar to the electric resistor $R = (\Delta V)/\Phi$. The reluctance depends on the length, the cross-section and the material constant of the flux carrying material. Applying Ampere's Law to the magnetic network leads to a set of algebraic equations $\Phi = R^{-1}\Delta V$, which can be solved for the unknown magnetic fluxes. With $B_{pole} = \Phi/A_{pole}$ and equation (1) follows the entire force of the magnetic bearing. For a given magnetic bearing geometry and material property, the network input data are the coil currents and the rotor positions. The analysis is computed using the assumptions of no flux fringing, no flux leakage and a uniform flux density in every flux-carrying cross-section. An advantage of this measurement technique is the extendability to consider nonlinear material behavior and hysteresis effects as described in e.g. Meeker et al. [8], Springer et al. [12]. Furthermore, additional sensors are again not necessary. However, the complexity of this method increases the computation time significantly. Hence, the method is only applicable for on-line implementation.

The resulting force error for this method can be seen in figure 6 for the same operation range as described above. The error is about 11%. As for the i-s-method, the main reason for the inaccuracies at higher loads are that the non-linearities of the magnetic material are not modelled. Hence, the network-method is

not superior to the i-s-method for the rotor in centric position, but is for eccentric rotor positions as clearly demonstrated in figure 6. When calibrating the network procedure the error can be further reduced to 8% as pictured in figure 7. The calibration is done by applying a constant correction factor minimizing the maximum force error in the entire operating range.

Hall Sensor Method

The most accurate method of determining the magnetic bearing forces is the direct measurement of the flux density B_{pole_i} by means of Hall sensors at each pole. Therefore, Hall sensors have been placed at each pole of the magnetic bearing in the air gap. The necessary calibration procedure of the Hall sensors is described in Knopf et al. [6]. Knopf reported a force error of 5% for the entire working range considered here. He further mentioned that the substantial part of the remaining force error results from an offset depending on the rotor position. Therefore, a rotor position dependent factor (k_{offset} = 75N/mm) is introduced to correct this offset error. Hence, the resulting force error is reduced to a maximum of 2.8% (fig. 7). If the rotor is only operated in the nominal center of the bearing, the force error of this method will lie clearly below 1%.

Non-linearities of the material, hysteresis effects, and saturation have almost no influence on the measurement error unlike the i-s-method, because these effects are causing a change of the flux density, and hence being accounted for. Another advantage is that the measurement location is much closer to the location where the force is actually acting. This means that influences of the amplifiers, coils, etc. are not falsifying the measurement. The entire computation can be performed on-line, again. On the other hand, additional sensors as well as an enlargement of the air gap are required. As a consequence of this, the maximum applicable magnetic force is reduced.

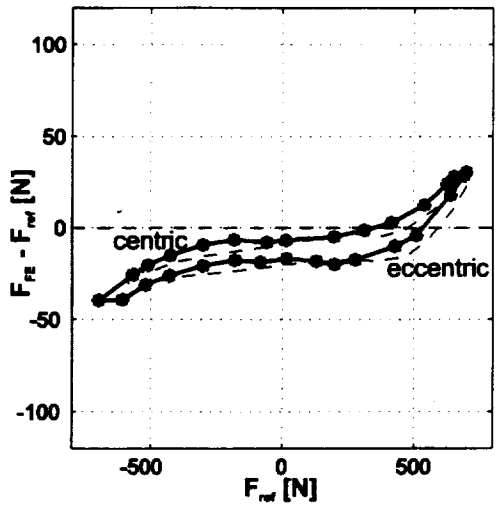

Figure 8. Force error of the FE-simulation for a centric (s_x=0mm, s_y=0mm) and an eccentric (s_x=0.3mm, s_y=0mm) rotor position.

FE-Model

For a more detailed knowledge about the magnetic flux density distribution in the magnetic bearings a Finite-Element model is generated using a commercial software package (FLUX2D). The deviations of the computed magnetic bearing forces compared to the measured ones are less than 5.6% for the same load cases applied before (fig. 8). These agreements confirm a good quality of the model. A further improvement of this performance requires an experimental determination of the exact material behavior (BH-curve), which is modelled so far based on manufacturer's specifications without hysteresis effects.

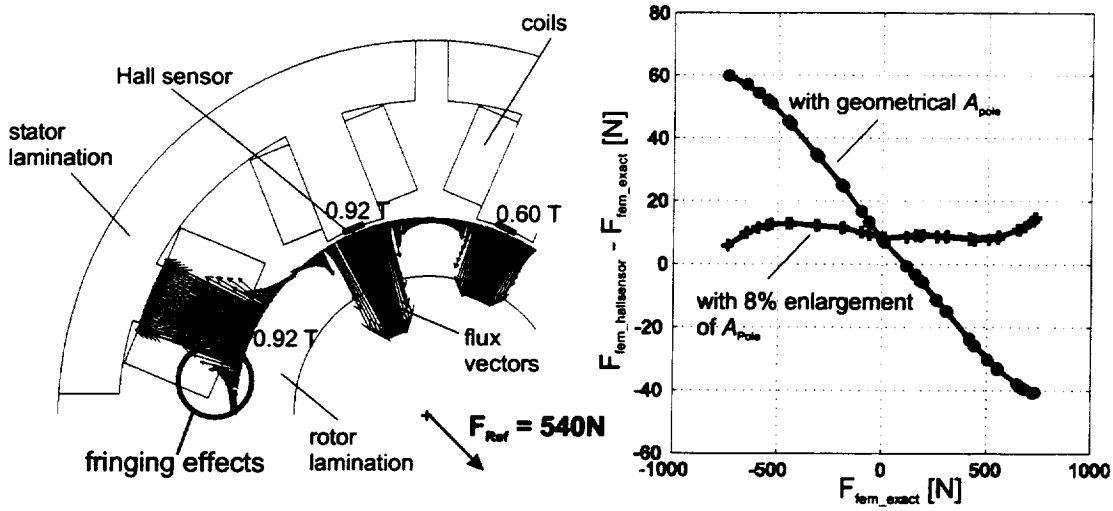

Figure 9. Left side: The magnetic flux distribution along the rotor lamination for an external force of 540N and centric rotor position shows the fringing effects.
Right side: Force measurement error of the simulated Hall sensor method for different external loads and centric rotor position.

With the FE-model the Hall sensor measurement technique is simulated. On one hand, the magnetic force is calculated from the integral of the flux values along the rotor. On the other hand, the magnetic force is computed using equation (1) from eight single flux values from the FE-simulation maintained at the Hall sensor locations. Assuming that the first calculation leads to the correct forces, the difference between both force computations represents the force error of the Hall sensor method. This error is shown in figure 9 for the centric rotor. If equation (1) is used with the geometrically calculated area of the magnetic poles, the resulting force error will be 9%. For getting more accurate results the pole area has to be increased by 8% due to the fringing effects in the air gap. This enlargement, independent of the load case and rotor position is accounted for through calibration and reduces the error significantly. The resulting error characteristic in the right picture of figure 9 agrees well with the one of the Hall sensor method in the left picture of figure 7. Only a general offset of about 10N yet remains in the FE-simulations. The dependence of the Hall sensor method on the rotor position could be observed, but with a smaller extend than with the measurement.

The different measurement techniques will now be used to diagnose various faults brought into the pump test rig. Especially, the accuracy obtained by the Hall sensor method seems to be sufficient for the diagnosis method, which is demonstrated in the following.

MODELING AND IDENTIFICATION

For many machines with rotating shafts the dynamic behavior can be described by linear models with time invariant system parameters. In these models the relation between input- and output quantities are

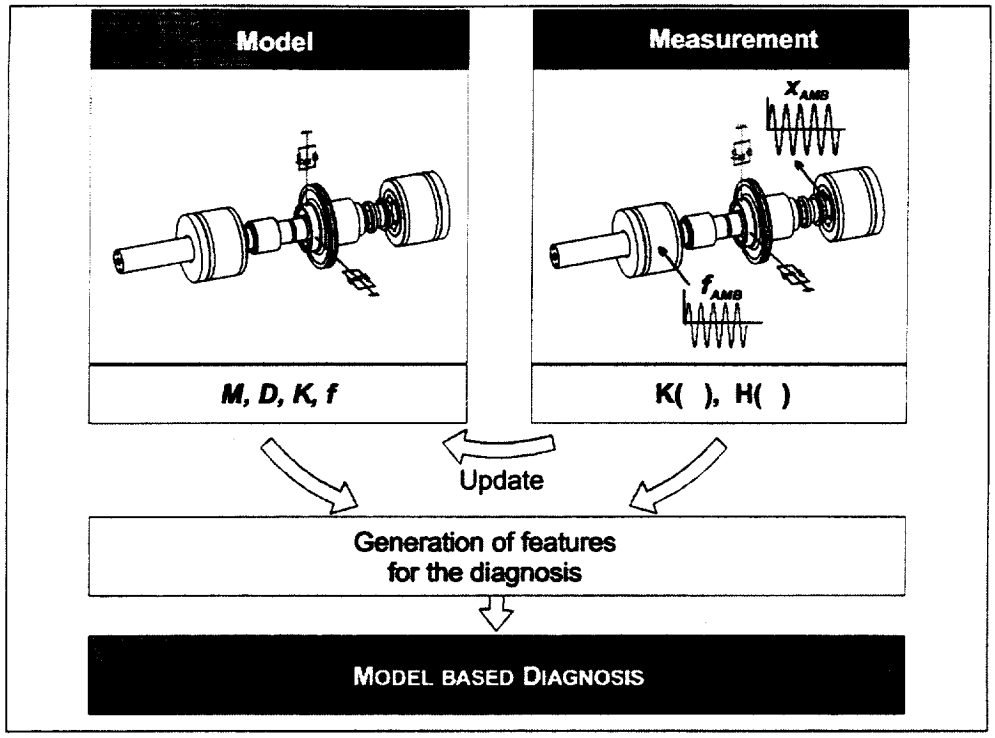

Figure 10. The procedure of the model based diagnosis using active magnetic bearings

given in terms of differential equations, expressing the dynamic equilibrium of inertia-, damping-, stiffness- and external forces:

$$\boldsymbol{M}\ddot{\boldsymbol{x}} + \boldsymbol{D}\dot{\boldsymbol{x}} + \boldsymbol{K}\boldsymbol{x} = \boldsymbol{f}. \tag{5}$$

The physical mass, damping and stiffness parameters, assembled in the nxn-system matrices $\boldsymbol{M}$, $\boldsymbol{D}$, $\boldsymbol{K}$, (n number of degrees of freedom), characterize the dynamic behaviour of the system. The determination of the physical parameters $\boldsymbol{M}$, $\boldsymbol{D}$, $\boldsymbol{K}$ is possible either by calculations or by measurements. The measurement procedure is known as identification. More precisely, if the structure of the rotordynamic model is already known, e.g. by equation (5), and only the parameters are not known and have to be identified, this is called parameter identification.

From the measured input and output signals the dynamic characteristics can be calculated from well-known input/output relationships in the time or in the frequency domain. In this paper only frequency domain relations will be treated. When input-output relations are considered, the following complex frequency response functions can be introduced

$$\hat{\boldsymbol{f}}(\Omega) = (\boldsymbol{K} - \Omega^2\boldsymbol{M} + j\Omega\boldsymbol{D})\hat{\boldsymbol{x}}(\Omega) = \overline{\boldsymbol{K}}(\Omega)\hat{\boldsymbol{x}}(\Omega), \tag{6}$$

$$\hat{\boldsymbol{x}}(\Omega) = (\boldsymbol{K} - \Omega^2\boldsymbol{M} + j\Omega\boldsymbol{D})^{-1}\hat{\boldsymbol{f}}(\Omega) = \overline{\boldsymbol{H}}(\Omega)\hat{\boldsymbol{f}}(\Omega), \tag{7}$$

where $\overline{\boldsymbol{K}}(\Omega)$ is the stiffness and $\overline{\boldsymbol{H}}(\Omega)$ is the compliance frequency response function, respectively. From a practical point of view, in most rotating systems it is more easy to measure compliance functions instead of stiffness functions. On the other hand, concerning the parameter estimation, there is a very sim-

ple linear relation between the physical parameters and the stiffness frequency function. The objectives of the measurement task are to excite a rotordynamic system artificially by force or kinematic excitation, to measure input and output signals and to process functions that are used for the parameter estimation and hence for the model updating (see fig. 10). In case of linear systems the frequency domain functions (equation (6) and (7)) are often used.

When input/output functions of the system have been measured, corresponding model functions are fitted to the measured ones in order to estimate the unknown physical parameters. In general, parameter estimation procedures like least squares method, instrumental variables, maximum likelihood can be used for this task.

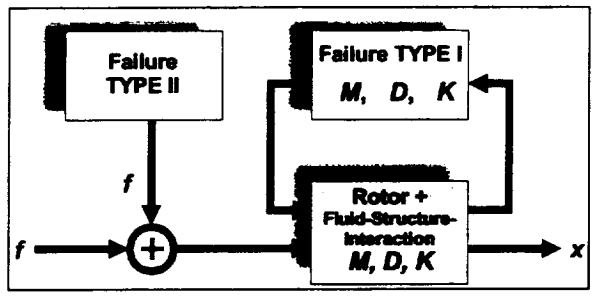

Figure 11. Scheme of the two different fault types being investigated

FAULT DETECTION AND DIAGNOSIS

Within this project several faults in the pump system will be identified. The aim of the project is to find out when a fault occurs and to determine the fault's type, location, and extent.

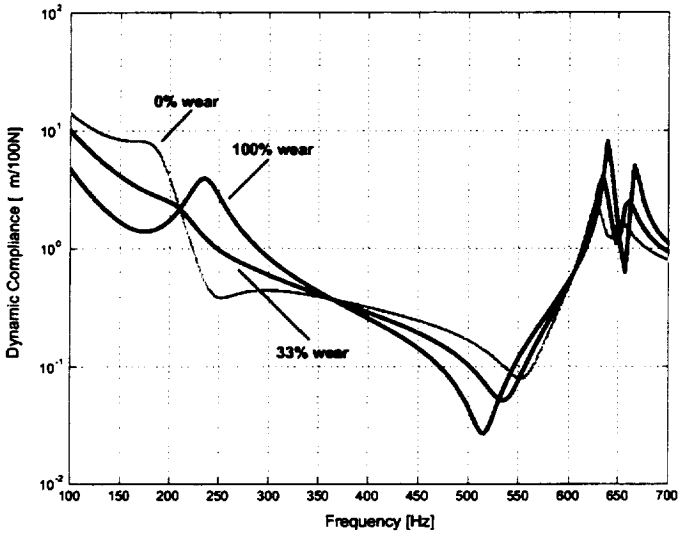

Figure 12. Change of the compliance function $\boldsymbol{H}(\Omega)$ due to different wear states of the balance piston.

In general, the faults brought into the system are subdivided in two cases. Faults of type I (see fig. 11) are altering the system matrices. These are for example a crack in the rotor, the wear of the seals, loosening parts, etc. Faults of type II are caused by changing external loads like an increase of the imbalance, cavitation, etc.

Exemplarily, some simulation results of the pump with different worn out states of the balance piston are presented. The different states are a seal with a clearance of 0.2mm (new), 0.3mm (33% wear), and 0.5mm (100% wear). The corresponding mass, stiffness, and damping coefficients for the simulation are calculated with validated programs, which are described in detail in [11]. Based on the models, it is possible to compute the resulting compliance functions $\boldsymbol{H}(\Omega)$ including the different seal states. Corresponding results are presented in figure 12. From this figure it can be derived that with an excitation amplitude of about 100N corresponding responses of about 5µm in the vicinity of the first and second eigenfrequencies can be expected. Hence, the location of the eigenfrequencies can be identified from the measured compliance function. Repeating this procedure for the different worn out

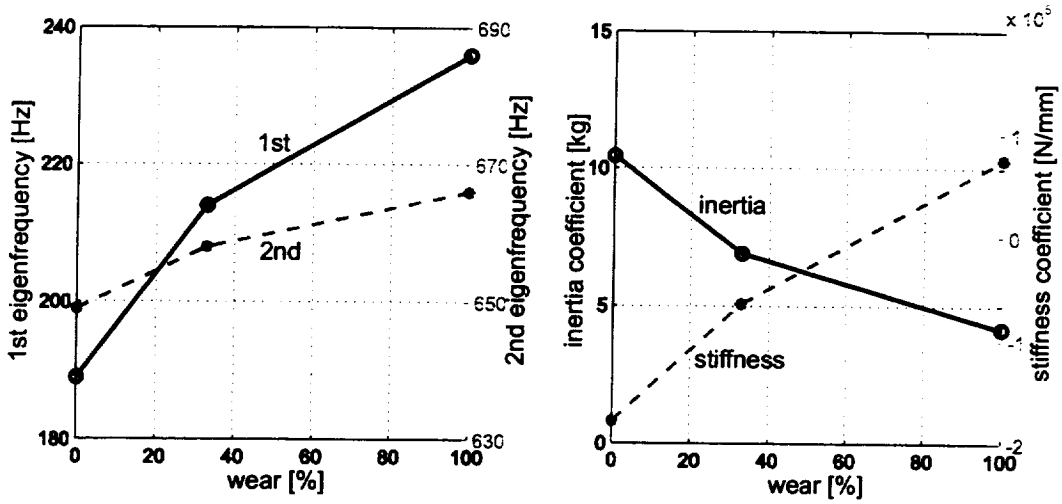

Figure 13. The change of two features characterizing the wear of the balance piston. On the left side, the increase of the first and second bending eigenfrequencies and on the right side, the altering of the identified inertia and stiffness coefficients.

states of the balance piston leads to the left picture in figure 12. The eigenfrequencies clearly increase with a wearing out piston due to decreasing inertia and damping forces in the seal.

Furthermore, with the parameter estimation using the compliance function $\boldsymbol{H}(\Omega)$ the seal coefficients can directly be derived. Exemplarily, the stiffness- and inertia coefficient are shown in the right picture of figure 13. With increasing wear of the balance piston the inertia coefficient decreases while the stiffness coefficient increases.

Conclusion and Outlook

In this paper the model based diagnosis using active magnetic bearings in a centrifugal pump is introduced. For this type of diagnosis using frequency response functions an accurate force measurement is crucial. The paper compares force measurement results and achievable accuracies of a radial magnetic bearing using different measurement techniques over a large operating range. The different techniques investigated are the i-s-method, a reluctance network method, and a Hall sensor method. For each method the accuracy as well as the ability for on-line computation and the improvement through calibration is presented. The most accurate method is the Hall sensor method. Additionally, a finite element model is generated to simulate this measurement technique. As a result of the simulation a rotor position dependent factor is introduced to account for the fringing effects. A future improvement of the Hall sensor measurement technique could be the development of a correction factor depending on the coil current and the rotor position for each pole instead of one for the whole bearing. Exemplarily, simulation results of a worn out balance piston of a single-stage pump are presented. The simulation shows that the accuracy of the force measurement achieved will enable the diagnosis of this fault in the pump system.

ACKNOWLEDGEMENT

The presented paper is a result from the work of the Special Research Program (SFB 241) sponsored by the German Research Council (DFG).

REFERENCES

[1] **D.O. BAUN, R.D. FLACK:** *A Plexiglas Research Pump With Calibrated Magnetic Bearings/Load Cells For Radial And Axial Hydraulic Force Measurement.* ASME Fluids Engineering Division Summer Meeting, FEDSM'97, June 22 -26, 1997.

[2] **P. FÖRCH:** *Dynamische Untersuchungen an rotierenden Strukturen mittels Magnetlagern.* Diss. Technische Universität Darmstadt. Darmstadt: 1998

[3] **C. GAEHLER:** *Rotor Dynamic Testing and Control with Active Magnetic Bearings.* Diss. Swiss Federal Institute of Technology Zürich. Zürich: 1998

[4] **R. ISERMANN** (Hrsg.): *Überwachung und Fehlerdiagnose.* Düsseldorf: VDI-Verl., 1994.

[5] **E. KNOPF, M. AENIS, R. NORDMANN:** *Aktive Magnetlager zur Identifikation der dynamischen Eigenschaften von mediumgeschmierten Gleitlagern.* thema FORSCHUNG, Volume 1/99, S. 80f, Hrsg. Präsident der TU-Darmstadt, Verlag für Marketing und Kommunikation, Worms, 1999.

[6] **E. KNOPF, R. NORDMANN:** *Active Magnetic Bearings for the Identification of Dynamic Characteristics of Fluid Bearings*, 6th International Symposium on Magnetic Bearings, Massachusetts Institute of Technology, Cambridge, USA, 1998

[7] **S. LEONHARDT:** Modellgestützte Fehlererkennung mit neuronalen Netzen - Überwachung von Radaufhängungen und Diesel-Einspritzanlagen. Diss. TH Darmstadt. Fortschritt-Berichte VDI Düsseldorf: VDI-Verlag, 1996.

[8] **D.C. MEEKER, E.H MASLEN, D.N. MYOUNGGYU:** *A Wide Bandwidth Model For The Electrical Impedance of Magnetic Bearings.* NASA conference publication No. 3336/PT2, 1996.

[9] **R. NORDMANN**: *New Identification Techniques in Rotordynamics Using Motion and Force Control.* MOVIC'98, Zurich, Switzerland, Aug. 25-28, 1998.

[10] **G. SCHWEITZER, H. BLEULER, A. TRAXLER:** *Magnetlager*, Springer Verlag, Berlin Heidelberg, 1994

[11] **J. SOBOTZIK, R. FONGANG, R. NORDMANN:** *Experimental Investigations on Fluid-Structure Interaction-Effects of a High-N_s Impeller.* Third International Conference on Pumps and Fans, Tsinghua University Beijing, Oct. 13 - 16, 1998.

[12] **H. SPRINGER, G. SCHLAGER, T: PLATTER:** *A Nonlinear Simulation Model For Active Magnetic Bearing Actuators*, 6th International Symposium on Magnetic Bearings, Massachusetts Institute of Technology, Cambridge, USA, 1998